SLOTTED-IN STEEL-PLATE CONNECTIONS FOR PANEL WALL ELEMENTS – EXPERIMENTAL AND ANALYTICAL STUDY

Per-Anders Daerga[1], Ulf Arne Girhammar[2], Bo Källsner[3]

ABSTRACT: This paper presents an experimental and analytical study of a steel plate connection for joining walls in the Masonite Flexible Building (MFB) system. These connections are used partly for splicing the wall elements and partly for tying down uplifting forces and resisting horizontal shear forces in stabilizing shear walls. The steel plates are inserted in a perimeter slot in the plyboard panel (a composite laminated wood panel) and fixed mechanically with screw fasteners. The load-bearing capacity of the slotted-in steel plate connections are determined experimentally and derived analytically for different failure modes. The test results show ductile post-peak load-slip characteristics, indicating that a plastic design method for shear walls can be applied to calculate the horizontal load-bearing capacity. The slotted-in steel plate connection concept can also be used for joining shear walls to transverse walls for tying down purposes in order to simplify the stabilization system of the building. The use of transverse walls for resisting uplifting forces introduces a three-dimensional behaviour of the wall junction and a more effective load transfer.

KEYWORDS: Slotted-in steel plate timber connections, timber wall elements, multi-storey timber building, Masonite Flexible Building system.

1 INTRODUCTION

The introduction of performance based design codes in Sweden 1994, opened for constructing timber buildings higher than two storeys. Since then, the construction of multi-storey timber buildings has developed rapidly due to new applications of construction types and building systems, reformulation of fire protection regulations and developments in sound insulation [1]. Today, timber construction technology is highly competitive regarding cost efficiency, sustainability, environmental impact, prefabrication processes and erection technique. The Masonite Flexible Building (MFB) system is one of several systems based on prefabricated units. The MFB system is a panel construction with load-carrying wall, floor and roof elements composed of composite beams, studs and panels mechanically joined with steel-plate connections [2]. In this paper, the slotted-in steel plate connection is studied. The sheet steel hanger is discussed in a companion paper [3].

[1] Per-Anders Daerga, PhD Student, Building Engineering, Faculty of Science and Technology, Umeå University, SE-901 87 Umeå, Sweden. Email: peranders.daerga@tfe.umu.se
[2] Ulf Arne Girhammar, Professor ,Timber Structures, Division of Structural and Construction Engineering, Luleå University of Technology, SE-971 87 Luleå, Sweden.
E-mail: ulf.arne.girhammar@ltu.se
[3] Bo Källsner, Professor, School of Engineering, Linnæus University, Lückligs Plats 1, SE-351 95 Växjö and SP Wood Technology – Technical Research Institute of Sweden, Stockholm. Email: bo.kallsner@sp.se

2 THE MASONITE FLEXIBLE BUILDING SYSTEM

The Masonite Flexible Building (MFB) system is a panel construction system developed for multi-story residential and public buildings. It encompasses plane units of wall, floor and roof elements, which all can be customized and prefabricated to a high degree of completion. The wall elements are structurally connected with slotted-in steel plates while the floor elements are suspended from the walls by sheet steel hanger connections, see Figure 1.

The structural skeleton of the elements consists of light-weight timber I-beams, I-studs and a composite laminated wood panel called plyboard, which are mechanically joined to form a ribbed panel structure. The plyboard panel is shown in Figure 2.

3 SLOTTED-IN WALL CONNECTION

The MFB system was initially designed with a steel pinned connection for vertical wall to wall assembling. Due to the high centre tolerance requirements for the pin and the low resistance with respect to withdrawal forces, alternative connection methods were investigated which led to a slotted-in steel plate connection with screw fasteners put in a perimeter slot in the plyboard panel.

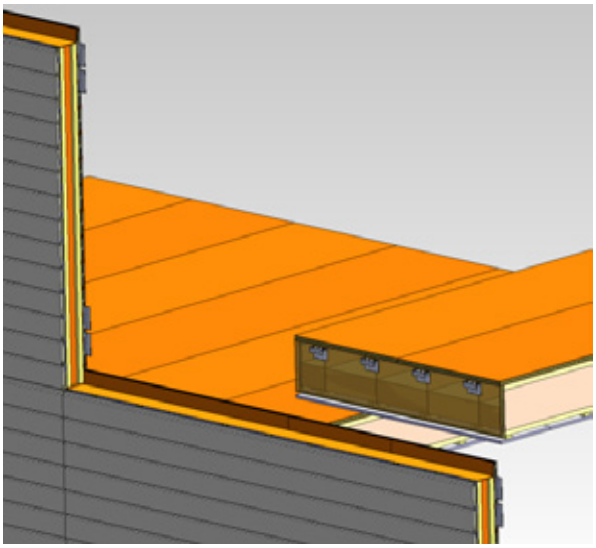

Figure 1. *External wall and floor units of the MFB XL system with wall-to-wall and floor-to-wall connections.*

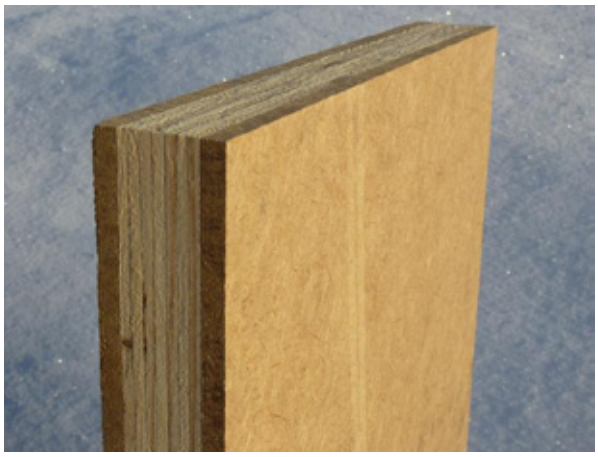

Figure 2. *Plyboard is a three-layered composite wood panel with a core of LVL and surface layers of hard fibre board. The panel is available in different thicknesses. The standard format is 1200x2400 mm.*

This arrangement provides design flexibility such that the number of plates and the screw configuration in the plate can be adapted to prevailing load conditions, and the perimeter slot allows for both vertical and horizontal splicing of wall elements. Figure 3 shows an external wall element with pre-mounted steel plates and screw connectors.

4 UPLIFT AND SHEAR TESTS

An initial experimental study was conducted to investigate the load-carrying capacity of the connection and the load-displacement relationship, especially the post-peak characteristics, to gain insight in the structural behaviour of the connection and get suggestions for improvements of the design. The test program included tests to simulate partly vertical uplift forces induced by wind forces and partly horizontal shear forces acting on a bracing wall according to Figure 11. The tested connections contained one (only uplift test), two and four screws as illustrated in Figure 4.

4.1 Experimental set-up

The experiments were conducted using a test rig with a closed-loop servo-hydraulic actuator with a force capacity of 100 kN in both tension and compression. The force was measured by a load-cell mounted on the actuator piston and the displacement of the connection was measured by an optical motion capture system. In both types of test, the specimens were loaded statically in displacement control mode with a rate of the actuator piston between 4 to 6 mm per minute. Figure 5 shows a rendered image of the test set-up for the uplift and the shear tests.

The uplift force was applied by inter-linked steel bars with pin connections to avoid restraints in the force chain and well defined boundary conditions, Figure 5a and c. The shear tests were conducted with a symmetrical specimen configuration as shown in Figure 5b and d. The force was applied through a rigid steel channel profile on the top surface of the middle specimen to achieve an evenly distributed pressure. To minimize the friction at the shear planes between the centre and the side pieces, flexible strips of PTFE foil (also known as Teflon) of thickness 0.25 mm was applied to the contact surfaces. The PTFE foils can be noticed in Figure 5c as light blue transparent strips on the shear planes.

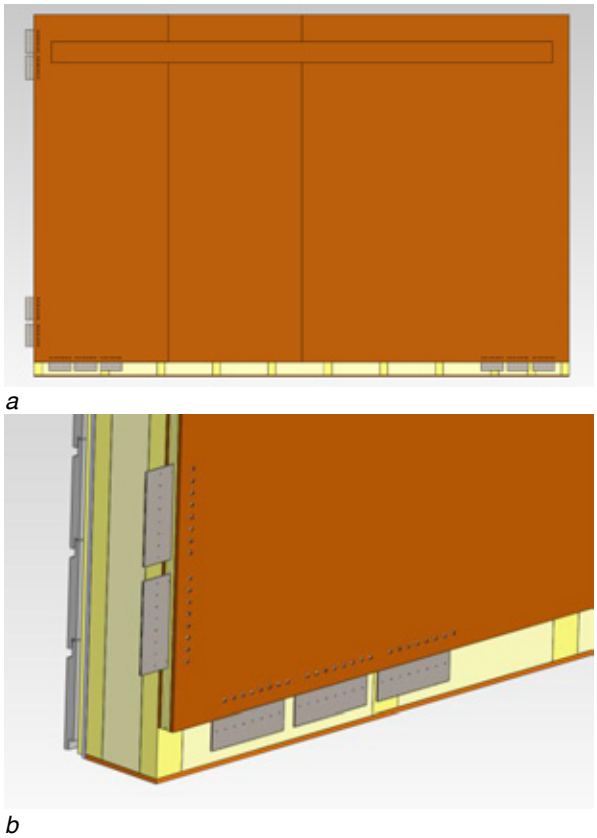

a

b

Figure 3. *An external wall element with slotted-in steel plate connections along bottom and left end edge: (a) front view, (b) view of left bottom part. The connections on the vertical end edge assist the connections along the bottom edge to resist uplift forces by being connected to transverse walls.*

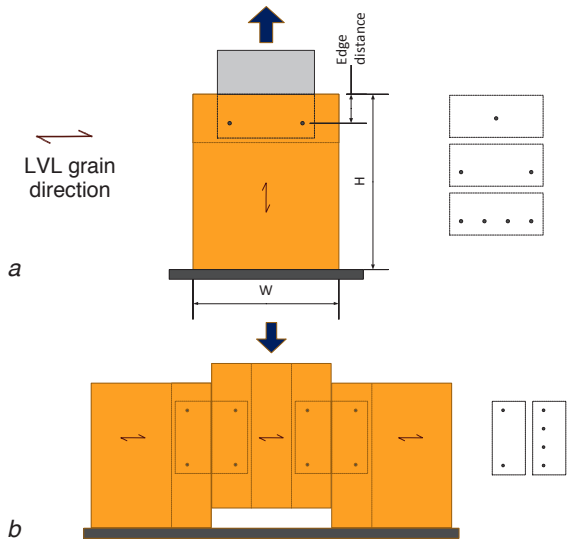

Figure 4. *Test set-up for simulation of: (a) vertical uplift force and (b) horizontal shear force (cf.Figure 11). Screw configurations shown to the right, edge distance 60 mm. Plyboard specimen 300×360×42 mm (w×h×t), steel plate 180×160×3 (w×h×t) of quality S355, frame screw 6,7×42 mm.*

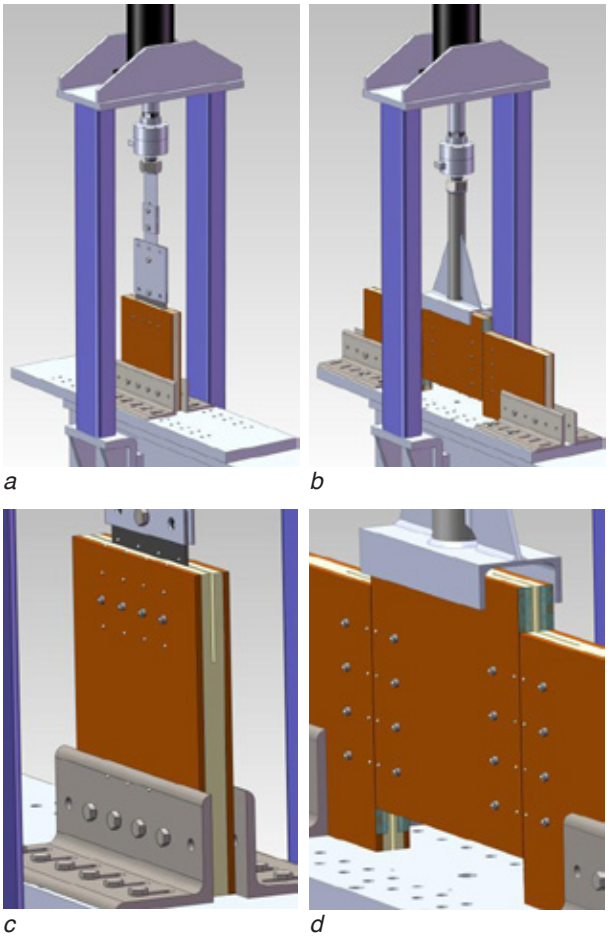

Figure 5. *Test arrangement: (a) Uplift test; (b) Shear test; (c) detail of uplift test showing screws and optical reference markers (white) attached to the steel plate, the plyboard surface and to the head of the screws; (d) detail of shear test with reference markers along the two shear planes and on the head of the screws.*

4.2 Optical displacement measurement

An optical motion capture system using high-speed infrared video cameras and passive markers attached to test object was used for measuring displacements. The measurement system is developed and marketed by Qualisys AB [4]. The employed system featured three Oqus cameras, lightweight reflex markers, an A/D-board for synchronously data acquisition of motion data from the cameras and analogue voltage data from the load-cell, and a motion capture software (QTM) for data processing and calculation of marker position. Each camera tracks and records the 2D-movement of the individual markers, and by processing the recorded data from several cameras three-dimensional trajectories of the individual markers are obtained. The particular markers used in the tests were plastic half spheres with a diameter of 4 mm. They were attached to the surface of the test object by double sided tape.

In the uplift tests the markers were attached to the top surface of the plyboard specimen and to the steel plate just above the joint line. Additional markers were also attached to the surface of the front board, on the head of the screws and on the foundation plate to get an absolute reference, see Figure 5c. The joint slip (the relative displacement between the markers on the steel plate and the markers on the plyboard top surface) was calculated from the marker trajectories. The accuracy of the displacement measurements is better than 0.1 mm.

In the shear tests the markers were attached pairwise, one on each side of the joint, along the two shear planes to measure the movement of the middle test piece relative to the side pieces, i. e. the joint slip parallel to the applied force direction. Additional markers were also attached to the head of the screws and on the foundation plate, see Figure 5d.

4.3 Materials and specimens

The plyboard specimens had dimensions 300×360 mm *(w×h)* and a thickness of 42 mm. The LVL core was 26 mm thick with 7 plies, the surface fibreboard lamellae were 8 mm. The slot width was 4 mm with a depth of 100 mm. The steel plate was of grade S355 with the dimension 180x160x3 mm *(w×h×t)*.

With respect to erection of the wall elements on site, it was initially thought that it would be rational to use self-drilling screws to combine drilling and fastening in one single operation. Different types of self-drilling screws were selected and their drilling capability was evaluated on the plyboard specimens with the steel plate inserted in the slot. The drilling was executed with a handheld screw driver. The outcome showed it was a difficult task to execute since the board surface was hard to penetrate and because of that the screws started to wobble resulting in enlarged and conical holes. The steel plate was even harder to penetrate and it was only one screw that could drill through the steel sheet. The concept of using self-drilling screws was therefore abandoned, instead predrilling and fastening was applied in sequential

operations which worked fine without any problems. The predrilling was done using a drill of 0.9*d* (the diameter of the screw). Finally a frame screw, brand name Adjufix, usually used for mounting door and window frames, was selected. The frame screw had the dimension 6,7×42 mm *(d×l)* and is marketed by Kartro [5].

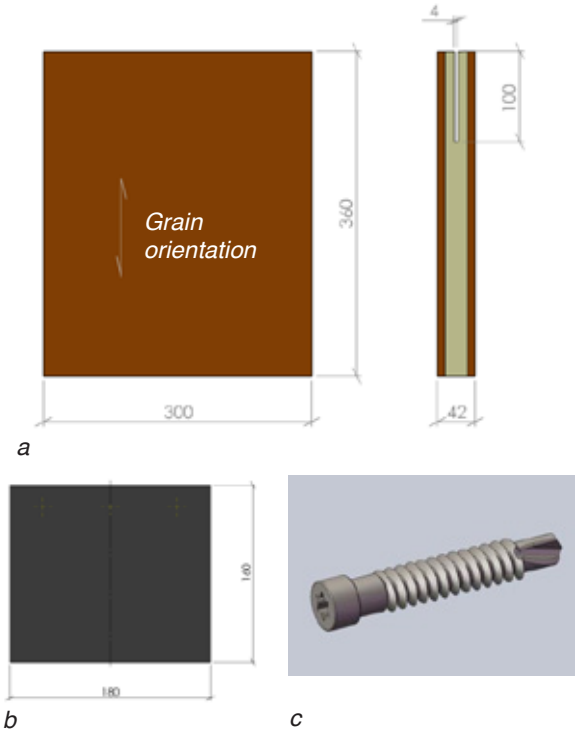

Figure 6. *(a) The plyboard specimen, 300x360x42 mm; grain orientation was vertical in the uplift tests and horizontal in the shear tests; (b) The steel plate, 180x 160x3 mm, quality S355; (c) The frame screw, self-drilling, brand name Adjufix, size 6,7x42 mm, d_{nom} = 6.7 mm, d_{eff} = 5.8 mm.*

5 TEST RESULTS AND EVALUATION

The average results of the uplift and shear tests are summarized in Table 1 and Table 2, and described in the following subsections. The results are evaluated with focus on the post-peak stage of the load-displacement relation since this influences the degree of ductility of the connections.

5.1 Uplift tests

The displacement is defined as the relative slip between the steel plate and the test specimen, i. e. the difference in vertical displacement of the markers on the steel plate just above the joint line and the markers on the top surface of the plyboard specimen, see Figure 5c.

The key to understand the failure mechanism of a connection with multiple screws is to understand the failure mechanism of the single screw connection. Hence, special attention is devoted to the failure process of the single screw connection.

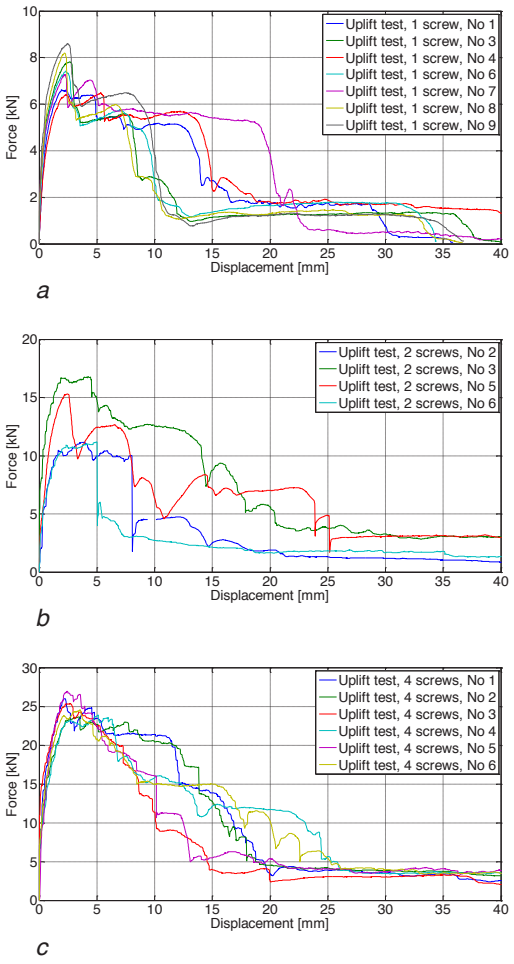

Figure 7. *Load-displacement graphs for the uplift tests with (a) 1 screw, (b) 2 screws and (c) 4 screws per connection.*

Table 1. *Test program and average result for uplift tests.*

Type of test	No of screws	No of tests	Ultimate load [kN]	Disp. at ult. load [mm]	Failure mode
Uplift	1	8	7,42	2,3	A
Uplift	2	4	13,7	3,9	B
Uplift	4	6	25,1	3,5	B

A Brittle failure of connection due to brittle bending failure of screw.
B Semi-ductile failure of connection due to successive failures of the fasteners and load redistribution in the remaining screws.

5.1.1 Single screw connection

Seven tests were conducted in total. Specimen No 2 was accidently destroyed during set-up and specimen No 5 was deliberately aborted at maximum load for later investigation of the failure mode. The maximum load varied between 6,46 to 8,62 kN with an average of 7,42 kN. The corresponding average displacement was 2,3 mm.

The load-displacement curves for the single screw connection are shown in Figure 7a. The ascending part of the curves is fairly linear up to the proportionality limit, which is about 40% of the maximum load, followed by a

gradual decrease in stiffness up to the maximum load. In the post peak stage, the course of failure followed the same pattern for all tests; a rapid load drop immediately after the maximum load followed by a plateau of variable length where the magnitude of load remained fairly constant or slightly increased until a second load drop occurred, from there on the load remained more or less constant to the end.

The interpretation of the characteristics of the load-displacement relation is as follows. The linear part of the ascending curve up to the proportionality limit is thought to correspond to elastic bending of the screw and elastic compression of the LVL due to embedment pressure from the screw. At the proportionality limit the embedment strength of the LVL is reached at the centre of the core due to high contact pressure exerted by the screw, and irreversible deformations start to develop with increasing loading as the plastic zone of the LVL core expands. This demonstrates as a nonlinear decrease in stiffness of the load-displacement relationship. When the maximum load is reached the bending strength of the screw is attained, and the LVL core is believed to have plasticized along the full length of the screw. The outer fibreboard layers are acting more or less as support for the screw and are believed to be essentially in an elastic state of stress (cf. failure mode e according to Figure 9).

When entering the post-peak stage the screw ruptures in a brittle way, which shows as a rapid load drop in the load-displacement curve with respect to the overall behaviour, but the broken screw parts are not yet fully detached but still exert pressure on the hole edges of the steel plate, enabling the load to remain constant or slightly increase with increasing displacement. The second load drop comes when the screw parts separate and the embedding stresses on the hole edges of the steel plate are discontinued. The residual strength is thought to be due to friction caused by the broken screw parts scratching on the surfaces of the steel plate.

Inspection of the broken screw parts after the tests were terminated showed that they were straight, giving support for a localized brittle bending failure at midspan of the screws. Also, scratch marks could be noticed on the steel plates supporting the explanation that the residual strength is due to friction between the broken screw parts and the steel plate.

5.1.2 Two screw connection

Six tests were conducted in total; four were executed successfully and two (No 1 and No 4) failed due to operation mistakes. The maximum load varied between 11,2 to 16,8 kN with an average of 13,7 kN. The corresponding average displacement was 3,9 mm.

As shown in Figure 7b, the individual curves display a rather large variation. Basically all the characteristic features of the single screw tests can be recognized also here, with the added arbitrariness in what order and what way the two screws failed successively.

5.1.3 Four screw connection

Six tests were conducted in total, all of them were executed successfully. The maximum load varied between 23,7 to 27,1 kN with an average of 25,1 kN. The corresponding average displacement was 3,4 mm.

The load-displacement curves are shown in Figure 7c. The ascending part of the curves is similar to the single screw tests, with a proportionality limit and a gradual decrease in stiffness up to the maximum load. The post peak part shows a gradual softening with minor load drops, indicating a failure process characterized by sequential bending failure of screws with some internal load redistribution.

5.1.4 Evaluation summary

The main difference between the single and the multiple screw connections is the ability of internal redistribution of the load for the latter type of connections, i. e. when the first screw reaches its load bearing capacity and starts to fail, its load share can be transferred to other screws which are able to carry additional loads. The load redistribution is governed by the failure mode of the screws, the screw pattern and the number of screws per connection.

From Table 1, it can be noted that the relative load-bearing capacity per screw decreases about 8 % for each doubling of the number of screws in the connection.

5.2 Shear tests

The shear tests show a rather high degree of ductility, both for a double and a four screw configuration, see Figure 8. As expected the individual scatter is less for connections with four screws than with two.

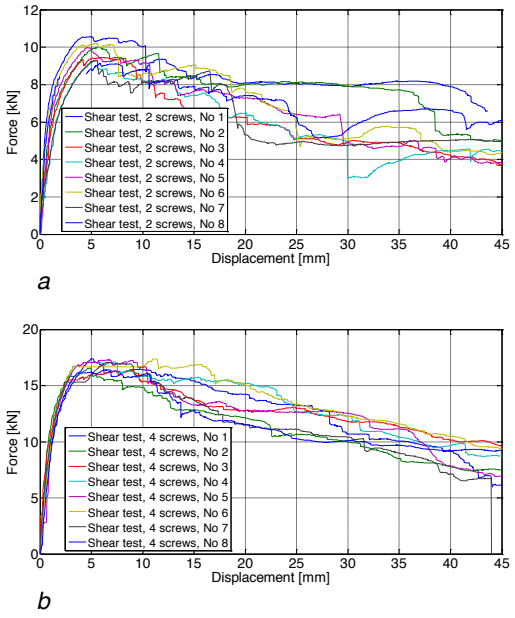

Figure 8. *Load-displacement graphs for the shear tests with (a) 2 screw and (b) 4 screws per connection.*

The average values for the ultimate load and corresponding displacement together with the failure

WCTE Auckland New Zealand 15 - 19 July 2012
World Conference on Timber Engineering

mode are summarized in Table 2. All specimens had ductile post-peak type of failure. The ultimate loadbearing capacity per screw was 13 % lower for the four screw connection compared with the double screw connection.

Table 2. *Test program and average result for shear tests.*

Type of test	No of screws	No of tests	Ultimate load [kN]	Disp. at ult. load [mm]	Failure mode
Shear	2	8	9,75	6,0	C
Shear	4	8	17,0	7,3	C

C. Ductile post-peak type of failure.

The experiments were conducted with specimens having a gap between the steel plate and the bottom of the slot of 10 mm. Due to the rotation the steel plate would come in contact at a displacement of about 10 mm. In reality, the steel plate will be mounted directly to the bottom of the slot. Therefore, the test results underestimate the real shear capacity.

The capacities for the shear tests are lower than those for the uplift tests, due to the eccentricity of the load transfer, see Section 7.1.1.

6 ANALYTICAL MODEL FOR THE SLOTTED-IN WALL CONNECTION

6.1 Yield model for lateral load-carrying capacity

The shear force capacity of the slotted-in wall connection can be analysed using the yield model of KW Johansens [6].

In the case of vertical uplift, the connection acts as a tie down anchored to the underlying wall or to the foundation, and in the case of horizontal shear the connection accomodates the shear load. In both cases, the fasteners are subjected to shear, although with different load to grain direction; at vertical uplift the force is acting parallel to the grain direction of the LVL core, Figure 4a (plastic tensile flow $f_{t,p}$ [N/m] in the connection), and for horizontal shear the force is acting perpendicular to the grain direction, Figure 4b (plastic shear flow $f_{s,p}$ [N/m] in the connection), see Figure 11. The hard fibreboard is assumed to have isotropic properties, i. e. independent of the force direction.

The following study is limited to the shear capacity of the connection. Failure modes depending on boundary effects such as edge and end distances, as well as tension, shear and splitting of the plyboard panel are not considered.

Consider the case with a thin metal plate, i. e. the thickness of the plate is less or equal to half the diameter of the fastener ($t_p \leq 0.5d$). Five failure modes are presented according to Figure 9 and the expression for the respective load-bearing capacity is given in the following. Other possible failure modes are not discussed.

6.1.1 Failure mode a - Embedment failure in the LVL core and the surface board layers

The failure load R_a corresponds to embedment failure in the LVL core and the surface board layers, and is derived from vertical equilibrium as

$$R_a = \left[2f_{h,b}t_b + f_{h,w}(t_w - t_s)\right]d \qquad (1)$$

where $f_{h,b}$ and $f_{h,w}$ are the embedment strength of the fibre board and the LVL core, respectively, d is the diameter of the fastener, other variables are defined according Figure 9a. The width of the slot is $t_s = t_p + 1$ mm.

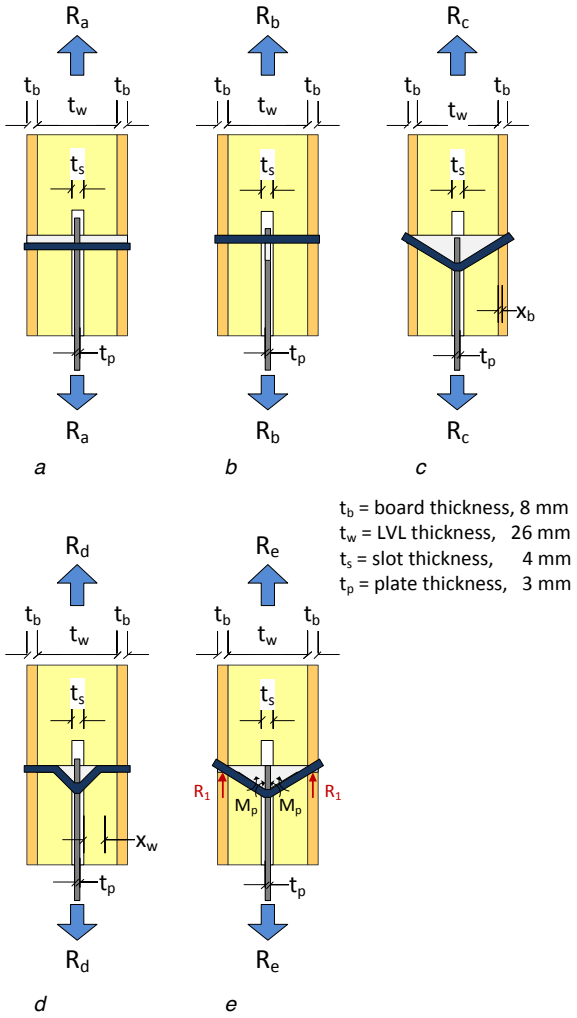

a Embedment failure in the LVL and the surface board layers.
b Embedment failure in the steel plate.
c Embedment failure in the LVL and the surface board layers, one plastic hinge in the fastener.
d Embedment failure in the LVL, two plastic hinges in fastener.
e Embedment failure in the LVL, board layers act as supports.

Figure 9. *Some failure modes for the slotted-in steel to timber connection. The force direction corresponds to vertical uplift. In the case of horizontal shear the force acts perpendicular to showed section although the failure mode is principally the same. The influence of edge and end distances is not considered.*

For the case of uplift force the embedment strength parallel to grain of the LVL core, $f_{h,w,0°}$, is used, and similarly for shear force, $f_{h,w,90°}$. With the notation

$$\gamma = \frac{f_{h,b}}{f_{h,w}} \quad (2)$$

Eq. (1) can be written

$$R_a = f_{h,w} t_w d \left[\left(1 - \frac{t_s}{t_w}\right) + 2\gamma \frac{t_b}{t_w}\right] \quad (3)$$

6.1.2 Failure mode b - Embedment failure in the steel plate

The failure load R_b corresponds to embedment failure in the steel plate. According to experiments, it is

$$R_b = 3 f_u t_p d \quad (4)$$

where f_u is the ultimate strength of the steel plate. The edge distance is assumed to be > *3d* to avoid any failure due to end or edge boundary effects.

6.1.3 Failure mode c - Embedment failure in the LVL core and surface board layers combined with a plastic hinge in the fastener

The failure load R_c corresponds to embedment failure in the LVL core and the surface board layers combined with a plastic hinge in the steel plate. It is derived from vertical equilibrium as

$$R_c = \left[f_{h,w}(t_w - t_s) + 2 f_{h,b} x_b - 2 f_{h,b}(t_b - x_b)\right] d \quad (5)$$

or

$$R_c = f_{h,w} t_w d \left[\left(1 - \frac{t_s}{t_w}\right) + 2\gamma \frac{t_b}{t_w}\left(2\frac{x_b}{t_b} - 1\right)\right] \quad (6)$$

Moment equilibrium at the centre of cross-section gives

$$M_p = \left[f_{h,w}\tfrac{1}{4}(t_w - t_s)^2 + f_{h,b} x_b \tfrac{1}{2}(t_w - t_s + x_b) - f_{h,b}(t_b - x_b)\tfrac{1}{2}(t_w - t_s + t_b + x_b)\right] d \quad (7)$$

which leads to

$$2\frac{x_b}{t_b} = \sqrt{(\gamma - 1)\left(\frac{t_w - t_s}{t_b}\right)^2 + 2\gamma\left(\frac{t_w - t_s}{t_b} + 1\right) + \frac{4M_p}{f_{h,w} d t_b^2}} - \frac{t_w - t_s}{t_b} \quad ; 0 < x_b < t_b \quad (8)$$

The load capacity is given by Eq. (6) together with Eq. (8). For the uplift force $f_{h,w} = f_{h,w,0°}$ and for the shear force $f_{h,w} = f_{h,w,90°}$.

6.1.4 Failure mode d - Embedment failure in the LVL core and double plastic hinges in the fastener

The failure load R_d corresponds to embedment failure in the LVL core and double plastic hinges in the steel plate. It is derived from vertical equilibrium as

$$R_d = 2 f_{h,w} x_w d \quad (9)$$

Moment equilibrium at halfway to the centre of the cross-section gives

$$2M_p = f_{h,w}\tfrac{1}{2} x_w^2 d \quad (10)$$

which leads to

$$x_w = 2\sqrt{\frac{M_p}{f_{h,w} d}} \quad ; 0 < x_w < \tfrac{1}{2}(t_w - t_s) \quad (11)$$

The loadbearing capacity becomes

$$R_d = 4\sqrt{M_p f_{h,w} d} \quad (12)$$

For uplift force $f_{h,w} = f_{h,w,0°}$ and for shear force $f_{h,w} = f_{h,w,90°}$ regarding the embedment strength of the LVL core.

6.1.5 Failure mode e - Embedment failure in the LVL core, surface board layers act as rigid supports

The failure load R_e corresponds to embedment failure in the LVL core while the surface board layers act as rigid supports. This mode is concluded from the experiments indicating that the board surface layers remained more or less intact without any signs of plastic deformations, hence suggesting that the board layers acted as rigid support for the screw. The embedment strength of the surface layers is about twice that of the LVL. Vertical equilibrium gives

$$R_e = 2R_1 + f_{h,w} d(t_w - t_s) \quad (13)$$

The vertical stress distributions in the fibre board layers balance each other. Moment equilibrium at the centre of the cross-section gives

$$R_1 \frac{t_w + t_b}{2} = M_p - f_{h,w} d\left(\frac{t_w - t_s}{2}\right)\left(\frac{t_w - t_s}{4} + \frac{t_s}{2}\right) \quad (14)$$

which leads to

$$R_1 = \frac{2M_p}{t_w + t_b} - \frac{1}{4} f_{h,w} d \frac{t_w^2 - t_s^2}{(t_w + t_b)} \quad (15)$$

Eq. (13) becomes

$$R_e = f_{h,w} d(t_w - t_s)\left[1 - \frac{1}{2}\frac{t_w + t_s}{t_w + t_b} + \frac{4M_p}{f_{h,w} d(t_w - t_s)(t_w + t_b)}\right] \quad (16)$$

Eq. (16) overestimates the loadbearing capacity due to some support displacement in the board layers, but underestimates it on the other hand somewhat due to the clamping effect of the screw head against the hard board layer.

For all the failure modes a-e, the axial force in the screw has been disregarded.

6.2 Strength values for plyboard and screw

The mean embedment strength of the fibre board and the LVL has been determined experimentally to 71 N/mm^2 and 49 N/mm^2, respectively [11].

The mean value of yield moment of the screw has been experimentally determined to 21.3 kNmm.

7 LOAD-BEARING CAPACITY

7.1 Lateral load-bearing capacity of fasteners

The experiments presented and described in Section 4 and 5, are compared with the derived analytical capacities of Section 6. For the uplift tests, the forces in the individual fasteners are readily given by the applied load. For the shear tests, however, the eccentricity in the load transfer between the mid and outer parts of the specimen needs to be accounted for.

7.1.1 Effect of eccentricity on fastener forces

Consider the shear tests in Figure 4b. The screw configuration for 2 and 4 screws are displayed in Figure 10. The eccentricity between the transferred shear force and the location of the fasteners give rise to a moment which introduces additional forces in the fasteners. Assume that all screws are completely plasticized.

Here a simple assumption is made concerning the statics of the load transfer between the mid and outer specimens. For the two screw configuration, the fastener reaction force due to the applied shear force F_s is determined from vertical equilibrium, and the fastener reaction force due to the eccentricity moment $F_s e$ is determined from moment equilibrium at the centre of gravity (cg) of the screw configuration. This gives

$$F_{y,p} = \frac{F_s}{2} \tag{17}$$

$$F_{x,p} = \frac{F_s e}{2s} \tag{18}$$

The resultant fastener force becomes

$$F_{e,2} = \sqrt{{F_{y,p}}^2 + {F_{x,p}}^2} = \frac{1}{2}F_s\sqrt{1+\left(\frac{e}{s}\right)^2} = F_{0,2}\sqrt{1+\left(\frac{e}{s}\right)^2} \tag{19}$$

where $F_{0,2}$ is the load on the fasteners from the shear load only. Similarly, the four screw configuration gives

$$F_{y,p} = \frac{F_s}{4} \tag{20}$$

$$F_{x,p} = \frac{3}{8}\frac{F_s e}{s} \tag{21}$$

$$F_{e,4} = \frac{1}{4}F_s\sqrt{1+\frac{9}{4}\left(\frac{e}{s}\right)^2} = F_{0,4}\sqrt{1+\frac{9}{4}\left(\frac{e}{s}\right)^2} \tag{22}$$

where $F_{0,4}$ is the load on the fasteners from the shear load only.

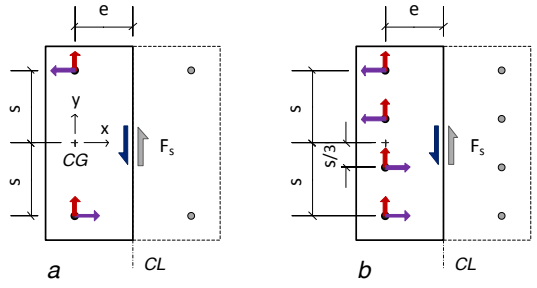

$F_{y,p}$ yield reaction force on fastener from shear force F_s

$F_{x,p}$ yield reaction force on fastener from eccentricity moment $F_s e$

CG Center of gravity of fastener group

CL Center line of shear plane

s Distance between outermost screw and CG, 75 mm

e Distance between shear force and CG, 60 mm

Figure 10. *Steel plate connection subjected to shear force according to Figure 4b: (a) Fastener forces for a two screw configuration, (b) Fastener forces for a four screw configuration.*

7.2 Experimental and analytical comparison

The geometrical values shown in Figure 6, Figure 9 and Figure 10 are: t_b = 8 mm, t_w = 26 mm, t_s = 4 mm, t_p = 3 mm, e = 60 mm, s = 75 mm, d_{nom} = 6.7 mm, d_{eff} = 5.8 mm. The density of the LVL is $\rho_{w,mean}$ = 424 kg/m^3.

According to Section 6.2 the embedment strengths are given by

$$f_{h,b,mean} = 71.0 \text{ N/mm}^2 \tag{23}$$

$$f_{h,w,mean} = 49.0 \text{ N/mm}^2 \tag{24}$$

which gives

$$\gamma = \frac{f_{h,b}}{f_{h,w}} = \frac{71.0}{49.0} = 1.45 \tag{25}$$

The yield moment is

$$M_p = 21.3 \text{ kNmm} \tag{26}$$

7.2.1 The uplift tests

The yield capacities for the different failure modes in the uplift tests are given in Table 1.

As pointed out earlier the value for mode e is somewhat under estimated with respect to the clamping effect at the ends, especially at the end of the screw head. If a linear stress distribution is assumed around the centre of the surface board layer and with a maximum stress at the outermost fibres equal to the embedment stress, $f_{h,b,mean}$ = 92.5 N/mm^2, the clamping moment at the ends of the screw can be estimated to 0.25M_p. If that moment is added the yield capacity of the connection increases from 6.00 to 6.63 kN for mode e.

Table 3. *Experimental and analytical shear capacities for the fastener in the uplift tests (loading parallel to grain).*

No of Screws (Config.)	Shear capacity per fastener [kN]			
	Uplift Test (Table 1)	Mode a R_a (Eq. 3)	Mode b R_b (Eq. 4)	Mode e R_e (Eq 16)
1	7.42	12.84	18.53	6.63
2	6.85	-	-	-
4	6.28	-	-	-

Failure mode c not applicable because $x_b > t_b$.
Failure mode d not applicable because $x_w > (t_w - t_s)/2$.

7.2.2 The shear tests

The eccentricity introduced by the shear load increases the load effect on the fasteners as shown in Eqs. (19) and (22). The failure load for the two and four screw configuration, respectively, are then given by

$$F_{0,2} \le \frac{R_i}{\sqrt{1+\left(\frac{e}{s}\right)^2}} \quad \text{[kN]} \quad ; 2 \text{ screws} \tag{27}$$

$$F_{0,4} \le \frac{R_i}{\sqrt{1+\frac{9}{4}\left(\frac{e}{s}\right)^2}} \quad \text{[kN]} \quad ; 4 \text{ screws} \tag{28}$$

where R_i is the capacity for governing failure mode *i* as given in Section 6.1. For the governing failure mode *e* (Eq. 16) the failure load becomes

$$F_{0,2} \le \frac{6.63}{\sqrt{1+\left(\frac{60}{75}\right)^2}} = 5.18 \quad \text{[kN]} \tag{29}$$

$$F_{0,4} \le \frac{6.63}{\sqrt{1+\frac{9}{4}\left(\frac{60}{75}\right)^2}} = 4.24 \quad \text{[kN]} \tag{30}$$

This should be compared with the ultimate shear load per fastener, equal to 4.88 kN (9.75/2) for the two screw configuration and 4.18 kN (16.72/4) for the four screw configuration, see Table 2 and Figure 8.

8 APPLICATION TO A STABILIZING WALL

8.1 Horizontal load-carrying capacity for shear walls with slotted-in connections

An analytical model based on the plastic lower bound method is applied for calculating the loadbearing capacity of a stabilizing wall panel with slotted-in steel plate connections with regard to vertical uplift and horizontal shear.

The horizontal loadbearing capacity of the shear wall is analysed using a plastic design method [7]. The so called static theorem states that a lower bound value of the capacity is obtained if all parts of the structure fulfil the conditions of equilibrium. A corresponding plastic design method has previously been developed for light-frame timber shear walls [10].

8.1.1 Basic assumptions

It is assumed that:

- the wall panel is rigid with respect to shear and buckling is prevented
- also the steel plate is rigid with respect to shear and buckling is prevented
- the slotted-in wall connections act as hinges

The horizontal load from wind induces vertical uplift forces at the windward side, vertical compressive forces at the leeward side and shear forces along the length of the wall, see Figure 11. The uplift forces are accommodated by the slotted-in connection and the compressive forces by contact pressure between the panel and the underlying wall panel or foundation. The eccentricity introduced because the horizontal shear forces act in the level of the fasteners in the connection, i. e. a distance above the bottom surface of the wall panel is neglected.

8.1.2 Force and moment equilibrium

Study the wall element shown in Figure 11. Force equilibrium in the horizontal direction gives

$$H = f_{s,p} l_{s,p} \tag{31}$$

Force equilibrium in the vertical direction gives the relation between the plastic tensile flow zone, i. e. the length of the connection plates, and the plastic compression flow zone in the wall panel

$$-f_{t,p} l_{t,p} + f_{c,p} l_{c,p} = 0 \tag{32}$$

$$l_{c,p} = \frac{f_{t,p}}{f_{c,p}} l_{t,p} \tag{33}$$

The total length of the connection plates is determined by studying the equilibrium of the wall around the lower right corner

$$Hh - f_{t,p} l_{t,p}\left(L - \tfrac{1}{2} l_{t,p}\right) + f_{c,p} \tfrac{1}{2} l_{c,p}^2 = 0 \tag{34}$$

By introducing the notations

$$\alpha = \frac{f_{t,p}}{f_{c,p}} \tag{35}$$

$$\beta = \frac{f_{s,p}}{f_{t,p}} \tag{36}$$

and using Eq. (34) to (36), an expression for the length of the connection plates is obtained:

$$l_{t,p} = \frac{L}{1+\alpha}\left[1 - \sqrt{1 - 2(1+\alpha)\beta \frac{h}{L}\frac{l_{s,p}}{L}}\right] \tag{37}$$

For the simplified assumption that the compressive reaction force, $R_c = f_{c,p} l_{c,p}$, is replaced by an equivalent point force acting on the bottom right corner, i. e.

$$l_{c,p} \to 0;\ f_{c,p} \to \infty \Rightarrow \alpha \to 0 \tag{38}$$

Eq. (37) simplifies to

$$l_{t,p} = L\left[1 - \sqrt{1 - 2\beta \frac{h}{L}\frac{l_{s,p}}{L}}\right] \tag{39}$$

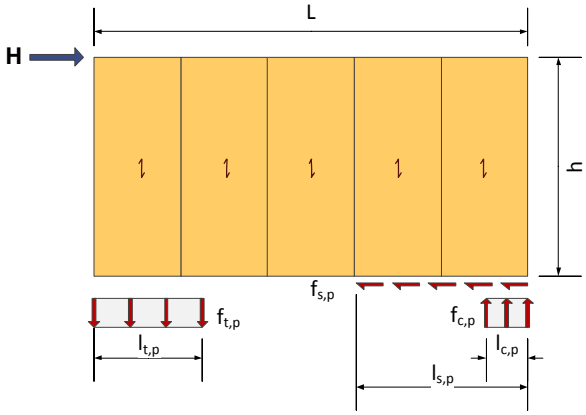

***Figure 11**. Force and moment equilibrium model for a rigid wall unit subjected to a horizontal wind force. The model is the base for the plastic lower bound method for calculating the loadbearing capacity of a panel wall element with slotted-in steel plate connections.*

8.1.3 Design procedure

The design of the wall connection can be done accordingly. The sufficient length of the plastic shear flow zone, $l_{s,p}$, when subjected to a horizontal load H is

$$l_{s,p} = \frac{H}{f_{s,p}} \tag{40}$$

The associated length of the plastic tensile flow zone is given by Eq. (37). There is no geometrical relationship between $l_{t,p}$ and $l_{s,p}$ except for the limitation

$$l_{t,p} + l_{s,p} \le L \tag{41}$$

The length of the plastic compression flow zone in the compressed side of the wall is given by Eq. (39).

8.2 The plastic capacity of the slotted-in connection

The plastic tensile flow strength, $f_{t,p}$, of the connection, i. e. the load-bearing capacity per unit length of the connection when subjected to an uplift force, is

$$f_{t,p} = \frac{nR_t}{b_t} \quad (42)$$

where R_t is the plastic uplift capacity per fastener for the governing failure mode, n is the number of fasteners in the connection, and b_t is the effective width of the connection perpendicular to the force direction. The uplift (tensile) force acts perpendicular to the bottom edge of the wall element, or, the row of fasteners. The maximum load attained in experimental uplift tests corresponds to nR_t.

The plastic shear flow strength, $f_{s,p}$, of the connection, i. e. the loadbearing capacity per unit length of the connection when subjected to a horizontal shear force, is

$$f_{s,p} = \frac{nR_s}{b_s} \quad (43)$$

where R_s is the plastic load-bearing capacity per fastener for the governing failure mode, n is the number of fasteners in the connection, and b_s is the effective width of the connection parallel to the force direction. The shear force acts parallel to the bottom edge of the wall element, or, the row of fasteners. The maximum load attained in experimental shear tests corresponds to nR_s.

8.3 Shear wall tied to transverse wall

The slotted-in steel plate connection concept can also be used for joining shear walls to transverse walls for tying down purposes in order to simplify the stabilization system of the building, see Figure 12 and Figure 3. The use of transverse walls for resisting uplifting forces introduces a three-dimensional behavior of the wall junction and a more effective load transfer.

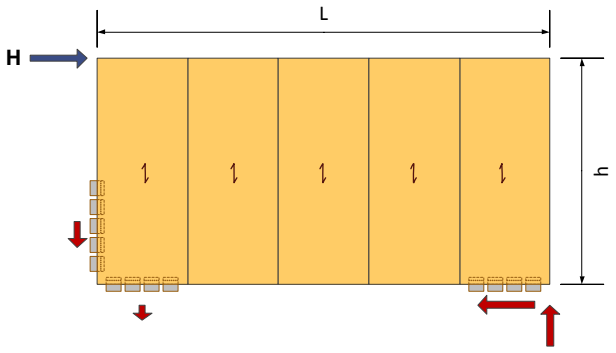

Figure 12. *Shear wall tied to transverse wall by adding slotted-in connection along the windward side.*

9 CONCLUSIONS

The experimental study on the slotted-in steel plate connection suggests that the concept can be efficiently used in stabilizing walls where the connections can be utilized for both tying down purposes and resist horizontal shear forces. The connections show acceptable ductile behaviour and promising load capacities to be used in multi-store buildings. The design needs to be investigated further with respect to the characteristics of the components in the connection in order to optimize the strength and stiffness.

The plastic analytical model for calculating the load-carrying capacity shows acceptable agreement with the experimental results and, therefore, is applicable to this kind of slotted-in connections. The ductile properties of the connection are sufficient for applying the plastic design method for shear walls.

ACKNOWLEDGEMENT

The authors thank the European Union's Structural Funds – The Regional Fund for its financial support.

REFERENCES

[1] Kolb J.: Systems in Timber Engineering. Birkhäuser Verlag AG, Basel Boston Berlin. In b11 Multi-storey timber buildings, pages 182–200, 2008.
[2] Daerga P. A., Girhammar U. A., Källsner B.: The Masonite Flexible Building System for Multi-Storey Timber Buildings. In: 12th World Conference on Timber Engineering, 2012.
[3] Daerga P. A., Girhammar U. A., Källsner B.: Suspended Floor Element Connections for the Masonite Flexible Building System. In: 12th World Conference on Timber Engineering, 2012.
[4] Qualisys AB. www.qualisys.se
[5] Kartro AB. www.kartro.se
[6] Johansen, K. W.: Theory of timber connectors. Proceedings of the International Association of Bridge and Structural Engineering (IABSE), Vol. 9, 1949, pp. 249-262.
[7] Neal, B. G.: Plastic methods of structural analysis. Chapman & Hall and Science Paperbacks, 2nd Edition, London, 1978.
[8] EN 1995-1-1:2004(E) – Eurocode 5 – Design of timber structures – Part 1-1: General – Common rules and rules for buildings. European Committee for Standardisation (CEN), Approved 2004-12-10 and published 2009-03-02.
[9] prEN 338:2008(E) – Structural timber – Strength classes. European Committee for Standardisation (CEN), June 2008.
[10] Källsner B., Girhammar U. A.: Plastic design of partially anchored wood-framed wall diaphragms with and without openings. In: Proceedings CIB-W18 Timber Structures Meeting, Dübendorf, Switzerland, Paper 42-15-1, 2009.
[11] Rios M.: Improved design of the element-to-element connector of the MFB-system (in Swedish). Master Thesis 293, Royal Institute of Technology, 2010.